

# SITTING VS STANDING: A COMPUTATIONAL COMPARISON OF HEMODYNAMICS IN CAROTID BIFURCATION

Maria Vittoria Caruso<sup>(a)</sup>, Raffaele Serra<sup>(b)</sup>, Paolo Perri<sup>(c)</sup>, Stefano de Francisci<sup>(d)</sup>, Gionata Fragomeni<sup>(e)</sup>

<sup>(a),(c)</sup>Bioengineering Group, "Magna Graecia" University, Catanzaro, 88100, Italy

<sup>(b),(c),(d)</sup>Operative Unit of Vascular Surgery, "Magna Graecia" University, Catanzaro, 88100, Italy

<sup>(a)</sup> [mv.caruso@unicz.it](mailto:mv.caruso@unicz.it), <sup>(b)</sup> [rserra@unicz.it](mailto:rserra@unicz.it), <sup>(c)</sup> [paolop83@yahoo.it](mailto:paolop83@yahoo.it), <sup>(d)</sup> [defranci@unicz.it](mailto:defranci@unicz.it), <sup>(e)</sup> [fragomeni@unicz.it](mailto:fragomeni@unicz.it)

## ABSTRACT

Sedentary lifestyle is very important in the etiology of atherosclerotic cardiovascular diseases. Furthermore, atherosclerotic plaques tend to occur near arterial bifurcation, as carotid one. Different studies have been conducted to investigate the physiological changes that occurred due to prolonged postural positions, but no computational analysis has been carried out. Aim of this study was to numerically explore the hemodynamic changes due to prolonged sitting or standing (1 hour respectively) in a carotid bifurcation, using the computational fluid dynamic (CFD) approach. In-vivo non-invasive measurements of anatomy, pressure field and velocity pattern were recorded in a cohort of 10 volunteers and used as boundary conditions for the simulations. The results showed that the worse hemodynamic profile occurs after sitting position near to the bifurcation - low velocity and wall shear stress (WSS), high stasis and chaotic flow - suggesting that a high risk of plaque formation and of stenosis could happen.

Keywords: carotid bifurcation, computational analysis, fluid dynamics, sitting, standing

## 1. INTRODUCTION

Atherosclerosis is the major cause of cardiovascular diseases (CVD), such as coronary heart disease, heart attack or stroke (Frostegard 2013). One important risk factor for its development is the lifestyle, which can favor plaque formation in the arteries in case of sedentary behavior, such as sitting or standing time. Indeed, prolonged sitting position is associated with CVD, but frequent short breaks in sedentary time may impart unique benefit (Owen et al. 2010), such as a significant reductions in postprandial glucose and insulin action (Dunstan et al. 2012).

The brain is perfused by means of the internal carotid arteries, vessels highly exposed to thromboembolic events (Malek et al. 1999), which can cause stroke. For this reason different studies have investigated what happens in these arteries considering different lifestyles and so, different postural positions. A comparison of waveforms in young, middle-aged and older groups has highlighted that regular aerobic exercise-trained increases velocity in respect to sedentary life in the

carotid artery (Azhim et al. 2007, Azhim et al. 2011). The sedentary time is also associated with an increase in carotid intima media thickness (IMT) (Kozàková et al. 2010, García-Hermoso et al. 2015) and the carotid stiffness and other cardiometabolic risk factors (Huynh et al. 2014). Furthermore, Krause et al. (2000) have found that prolonged standing at work is correlated with the progression of atherosclerotic events in the carotid bifurcation, in terms of increase of IMT.

The effects of posture has been also investigated in the brachial and femoral arteries (Newcomer et al. 2008), showing that, comparing the standing and sitting positions, the heart rate and blood flow are higher and the mean arterial pressure (MAP) is lower in both arteries.

Although postural changes have been much investigated from clinical view point, no studies have been carried out regarding the hemodynamics. So, a detailed analysis is necessary.

The objective of this study was to examine the hemodynamic changes in the carotid bifurcation due to prolonged sitting and standing time (1 hour respectively) by means of the computational fluid dynamics (CFD). This numerical approach allows to study, in time and in space, the two hemodynamic variables - the pressure field and the velocity pattern - resolving the governing equations by means of a numerical approach (simulations) (Tu et al. 2007). In-vivo non-invasive pressure and velocity measurements (Van de Vosse and Stergiopoulos 2011) were used as input for the simulations.

## 2. MATERIAL AND METHODS

### 2.1. Subjects

The subjects were 10 healthy volunteers, 5 men and 5 women, which didn't have cardiovascular diseases. Furthermore, the cohort has  $29.3 \pm 0.07$  years and a BMI of  $22.90 \pm 2.72$  kg/m<sup>2</sup>.

### 2.2. In-vivo measurements

The caliber of vessel and the velocity profile after 1h of sitting (case A) and after 1h of standing (case B) were recorded in the common carotid artery (CCA) and internal carotid artery (ICA) by means of the Hitachi-Aloka ProSound F37 ultrasound system (Hitachi Aloka

Medical America, Inc.). Starting on these data, the flow profile was calculated.

An applanation tonometry was used to record the pressure in the external carotid artery (ECA).

In all cases, the mean value and the standard deviation were evaluated. The diameter and the velocity at peak systolic and end diastole in sitting time and in standing one are reported in Table 1, 2 and 3 respectively. Pressure values in systolic peak and at end diastole and the MAP in the two cases are reported in Table 4.

### 2.3. CFD model

#### 2.3.1. Geometrical model

A carotid bifurcation was reconstructed by means of the segmentation process from CT images of a 30 years old man, done for clinical reasons, using Invesalius open source software. The geometry included the common carotid artery (CCA), the internal carotid artery (ICA) and the external carotid artery (ECA) (Figure 1). Starting from this 3D model, a new idealized model was reconstructed considering the centerlines of the patient-specific bifurcation in order to obtain the real bendings of the vessel. The diameter variation was modeled hypothesizing a circular shape. Furthermore, the mean value, obtained considered the 10 volunteer, was set for CCA and ICA caliber of the idealized model (Table 1). The ECA diameter value was chosen from the patient-specific model.

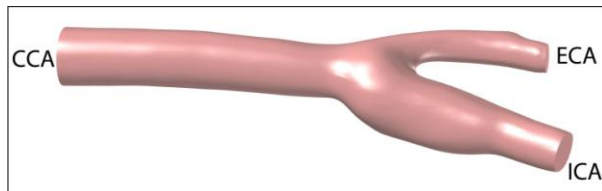


Figure 1: Geometrical idealized model of carotid bifurcation

Table 1: CCA and ICA diameter values for each volunteer, measured with the ultrasound system

Patient	Diameter [mm]	
	CCA	ICA
1	6.30	4.90
2	6.50	4.20
3	6.00	4.60
4	6.20	4.10
5	6.80	4.00
6	6.20	4.70
7	6.40	4.50
8	6.80	4.40
9	5.80	4.80
10	6.00	4.80
<b>Mean</b>	6.30	4.50
<b>SD</b>	0.33	0.32

Table 2: Velocity value in systolic peak for each patient in sitting position and in standing one.

Patient	Systolic Velocity [cm/s]			
	Sitting		Standing	
	CCA	ICA	CCA	ICA
1	35	20	39	22
2	32	20	41	28
3	30	15	38	21
4	40	23	44	24
5	35	25	39	29
6	42	20	46	24
7	48	28	50	30
8	32	21	38	26
9	38	18	50	22
10	36	17	49	23
<b>Mean</b>	36.80	20.70	43.40	24.90
<b>SD</b>	5.41	3.83	5.04	3.18

Table 3: Velocity value at end diastole for each patient in sitting position and in standing one.

Patient	Diastolic Velocity [cm/s]			
	Sitting		Standing	
	CCA	ICA	CCA	ICA
1	15	8	17	9
2	16	10	19	12
3	14	7	17	9
4	17	10	20	12
5	18	13	21	14
6	16	8	19	10
7	18	11	20	13
8	17	12	20	14
9	15	6	17	8
10	13	6	17	9
<b>Mean</b>	15.90	9.10	18.70	11.00
<b>SD</b>	1.66	2.47	1.57	2.26

#### 2.3.2. Mathematical model of blood flow

To study the hemodynamics from a macroscopic point of view, the blood can be modeled as an incompressible fluid with a density of  $1,060 \text{ kg/m}^3$  (Cutnell and Johnson 1998) and a Newtonian behavior, with viscosity equal to  $0.0035 \text{ Pa}\cdot\text{s}$  (Yilmaz and Gundogdu 2008). Furthermore, blood flow was hypothesized as laminar and 3D Navier-Stokes equations were used as governing laws:

$$\nabla \cdot \mathbf{u} = 0 \quad (1)$$

$$\rho (\partial \mathbf{u} / \partial t) + \rho (\mathbf{u} \cdot \nabla) \mathbf{u} = \nabla \cdot [-p\mathbf{I} + \mu(\nabla \mathbf{u} + (\nabla \mathbf{u})^T)] \quad (2)$$

Table 4: Pressure evaluated for each patient (P) in sitting and standing, considering the systolic peak (S), the end diastole (D). The mean arterial pressure (MAP) is also reported.

Pressure [mmHg]						
P	Sitting			Standing		
	S	D	MAP	S	D	MAP
1	110	75	86.67	95	70	78.33
2	130	80	96.67	120	75	90.00
3	110	75	86.67	95	65	75.00
4	120	70	86.67	100	65	76.67
5	120	95	103.33	110	75	86.67
6	110	70	83.33	95	65	75.00
7	120	80	93.33	105	70	81.67
8	125	80	95.00	115	70	85.00
9	120	70	86.67	110	60	76.67
10	120	85	96.67	105	70	81.67
<b>Mean</b>	118.50	78.00	91.50	105.00	68.50	80.67
<b>SD</b>	6.69	7.89	6.40	8.82	4.74	5.22

### 2.3.3. Boundary conditions

The CCA flow waveform was assumed as an inlet boundary condition, whereas the ICA flow waveform was set as an outlet boundary conditions, considering in both cases a fully developed steady profile (Poiseuille). Furthermore, the pressure waveform was applied as outlet boundary condition in ECA.

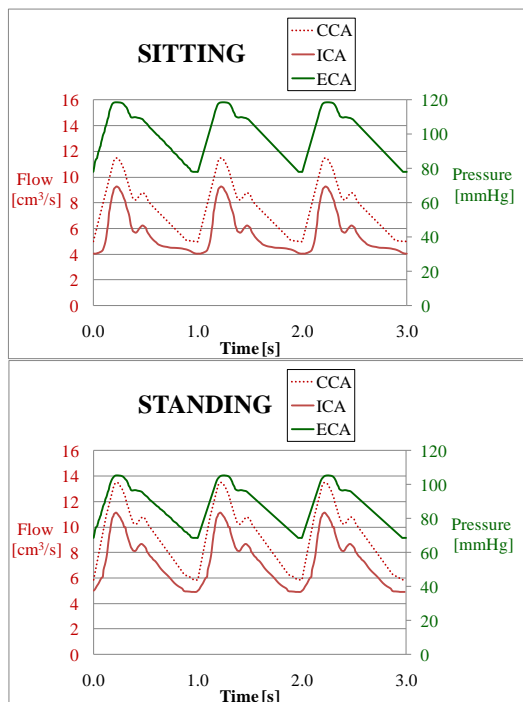


Figure 2: Boundary conditions in sitting position and in standing one.

### 2.3.4. Simulation details

The carotid bifurcation was discretized with tetrahedral, prism, triangular and quadrilateral elements. Moreover, in order to obtain accurate and grid independent solutions, the mesh was modeled so that the grid error - evaluated as:

$$e = |(Q_{in} - Q_{out}) / Q_{in}| \cdot 100 \quad (3)$$

where  $Q_{in}$  is the mean flow in inlet (CCA) and  $Q_{out}$  is the mean flow in outlet (ECA+ICA) - was less than 1%. According to the continuity equation (2),  $Q_{in} = Q_{out}$ , so the error evaluated with (3) is correlated to the grid. Moreover, considering a mesh of 65,063 total elements, the flows are  $Q_{CCA} = 7.69 \text{ cm}^3/\text{s}$ ,  $Q_{ICA} = 5.59 \text{ cm}^3/\text{s}$ ,  $Q_{ECA} = 2.09 \text{ cm}^3/\text{s}$ , so  $e = 0.13\%$ .

The CFD analysis was carried out using COMSOL 5.0 (COMSOL Inc, Stockholm, Sweden), a finite-element-based commercial software package. In both situations, time-dependent simulations were implemented, considering a time step of 0.001 s and using the direct solver Pardiso and the BDF method for the time stepping. Furthermore, the elements used in the finite element formulation were linear for both the velocity components and the pressure field (P1+P1).

### 2.3.5. Atherosclerotic parameters

Atherosclerosis is highly influenced by shear stress generated at the interface between blood and artery wall (Malek et al. 1999), known as wall shear stress (WSS). It can be evaluated as:

$$WSS = \sqrt{(\tau_x)^2 + (\tau_y)^2 + (\tau_z)^2} \quad (4)$$

where  $\tau_x$ ,  $\tau_y$  and  $\tau_z$  are the viscous stress in x, y and z directions, respectively. WSS is a time-dependent parameter, so the average over one cardiac cycle (T) can be evaluated, known as time average WSS (TAWSS):

$$TAWSS = 1/T \cdot \int_0^T |WSS| dt \quad (5)$$

Physiological level of TAWSS in arteries is in the range 1.5 - 2 Pa (Malek et al. 1999).

Another parameter linked to the shear stress is the oscillatory shear index (OSI), which reveals the overall WSS vector oscillation:

$$OSI = 0.5 \cdot \{1 - [(\int_0^T WSS dt) / \int_0^T |WSS| dt]\} \quad (6)$$

It varies from 0 to 0.5 and it is a dimensionless measure: the zero value indicates that there is no WSS variation (orderly and unidirectional flow), while 0.5 indicates a variation of 180° accordingly to a purely unsteady and chaotic flow with zero WSS (Dong et al. 2013). Moreover, it was demonstrated that this mechanical indicator is a good predictive parameter of plaque site (Knight et al. 2010).

The values of TAWSS and OSI are combined in relative residence time (RRT) parameter, expressed as:

$$RRT = [(1 - 2 \cdot OSI) \cdot TAWSS]^{-1} \quad (7)$$

that expresses the residence time of particles near the wall (Lee et al. 2009).

Atherosclerosis plaque can arise when the flow is disturbed and this area can be identified considering

$WSS \leq 0.481 \text{ Pa}$ ,  $OSI \geq 0.145$  and  $RRT \geq 2.944 \text{ Pa}^{-1}$  (Lee et al. 2008).

### 3. RESULTS AND DISCUSSION

#### 3.1. Flow and pressure waveforms

The flow waveform in CCA, ECA and ICA in sitting and in standing time is shown in Figure 3. In standing position the CCA and ICA flows are higher than the flows in sitting situation, with a mean increase of about 17.50% and 21% respectively. Furthermore, since the ICA mean flow percentage in respect to the CCA flow is about 80% in sitting and about 82% in standing, the flow in ECA is similar after the two postural situations. Regarding the pressure field, its distribution is similar in the three vessels (ICA, ECA and CCA) both in sitting and in standing situation (Figure 4) because the carotid bifurcation has a small length. Moreover, MAP is lower of about 11.84% in standing position respect to the sitting one.

#### 3.2. Velocity pattern

To analyze in details the velocity pattern during sitting (A) and standing (B), the streamlines of the velocity magnitude in systolic peak and at end diastole are reported in Figure 5 and 6 respectively. Furthermore, two different views - frontal (1) and posterior (2) - are considered. In both postural positions, chaotic flow occurs in the ICA in correspondence of bifurcation (carotid bulb), both in systole and in diastole. This swirling pattern is more emphasized in sitting, where flows are lowest. Moreover, in this area of bifurcation, the velocity values are near 0 m/s. This suggests that blood stasis characterizes this region.

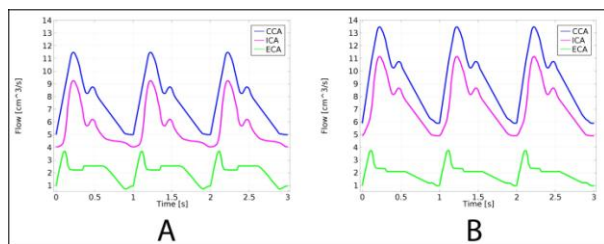


Figure 3: Flow waveforms in CCA, ICA and ECA during sitting (A) and standing (B)

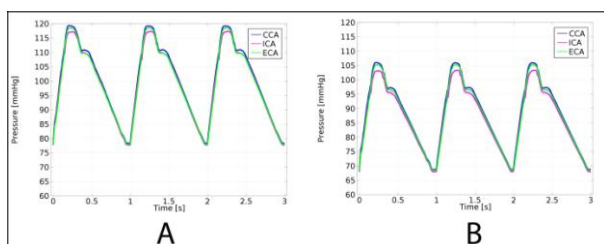


Figure 4: Pressure waveforms in CCA, ICA and ECA during sitting (A) and standing (B)

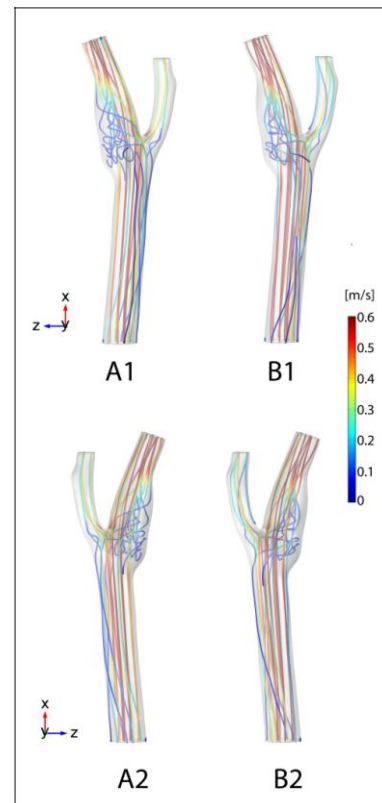


Figure 5: Streamlines of velocity magnitude at systolic peak during sitting (A) and standing (B), considering the frontal (1) and posterior (2) views.

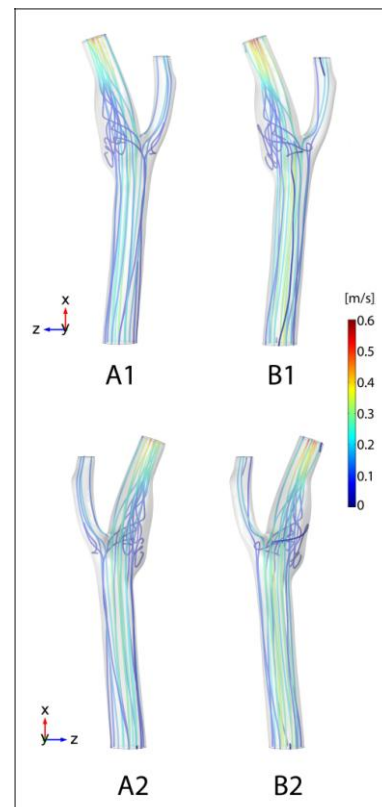


Figure 6: Streamlines of velocity magnitude at end diastole during sitting (A) and standing (B), considering the frontal (1) and posterior (2) views.

### 3.3. Hemodynamic parameters

The TAWSS distribution in sitting and standing is reported in Figure 7. Low WSS values are obtained in the bifurcation in correspondence of the carotid bulb, where stasis occurs. The worse TAWSS behavior happens in the sitting case, because a big area presents very low WSS, with zero value in some points (A1).

Moreover,  $WSS \leq 0.4 \text{ Pa}$  is associated with IMT (Glor et al. 2003), so in this case there is a high probability of wall thickening.

To investigate the flow pattern and its directionality, in terms of orderly or chaotic flow, unidirectional or retrograde flow and, consequently, WSS oscillation, the OSI pattern is illustrated in Figure 8. Common features among the two postural positions are that high values are recorded in the bifurcation in correspondence of the emergence of ECA and in the final area of carotid bulb, so the flow is swirling in all time of the cardiac cycle, and that 0 OSI characterized the remain areas, suggesting that orderly flow characterized these regions in the cardiac cycle. In sitting position the areas with  $OSI \geq 0.145$  are more extensive, so the carotid has a higher predisposition to endothelial dysfunction and atherogenesis (Ku et al. 1985) in this case.

Finally, the RRT was evaluated and its distribution considering 1 cardiac cycle is shown in Figure 9. During prolonged sitting, high time characterizes the bifurcation and the carotid bulb, whereas the remain regions of carotid artery is exposed to low RRT. On contrary, only few points present high RRT ( $10 \text{ Pa}^{-1}$ ) in standing position.

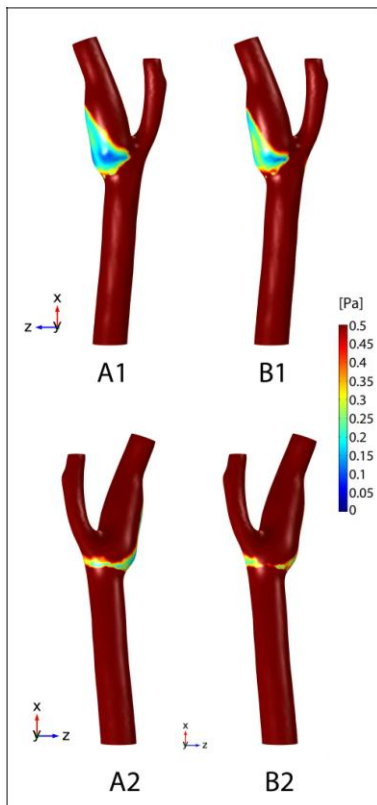


Figure 7: TAWSS during sitting (A) and standing (B), considering the frontal (1) and posterior (2) views.

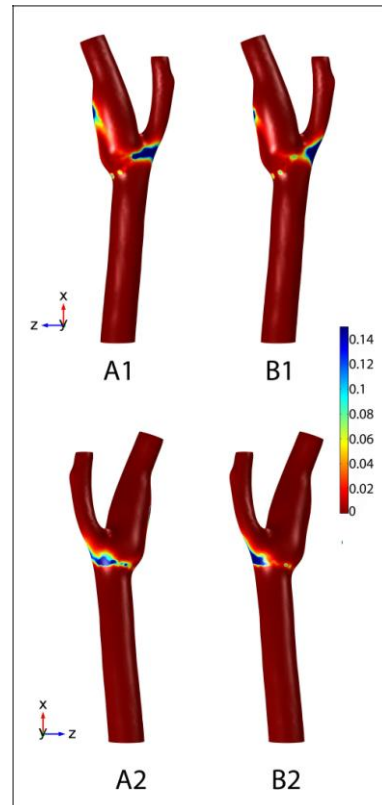


Figure 8: OSI during sitting (A) and standing (B), considering the frontal (1) and posterior (2) views.

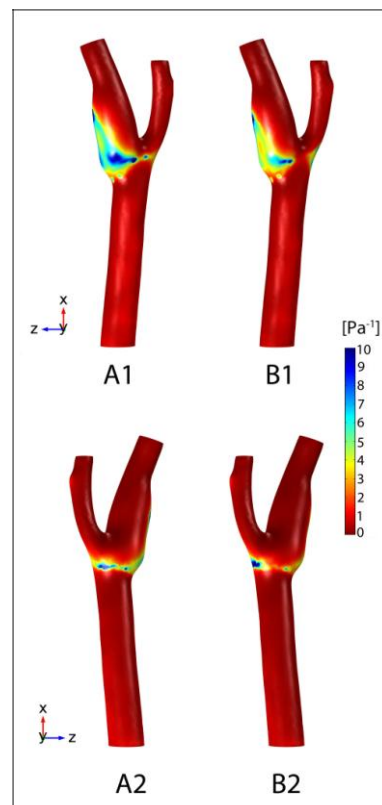


Figure 9: RRT during sitting (A) and standing (B), considering the frontal (1) and posterior (2) views.

Moreover, the atherogenic endothelial phenotype is promoted in the areas with TAWSS  $\leq 0.4$  Pa and RRT  $\geq 10$  Pa<sup>-1</sup> (Malek et al. 1999, Lee et al. 2009), so the worse situation occurs after prolonged sitting.

#### 4. CONCLUSION

This computational study provides detailed information regarding the hemodynamic changes that occurred in the carotid bifurcation considering prolonged sitting and standing. The numerical results suggest that the carotid bulb is the most atherosclerosis susceptible location both for the sitting and the standing position. Furthermore, the worse hemodynamic profile is generated after prolonged sitting time, suggesting that a high risk of plaque formation and, consequently, of stenosis could happen.

#### REFERENCES

- Azhim A., Katai M., Akutagawa M., Hirao Y., Yoshizaki K., Obara S., ... and Kinouchi, Y., 2007. Exercise improved age-associated changes in the carotid blood velocity waveforms. *J. of Biomed. & Pharm. Eng.*, 1, 17-26.
- Azhim A., Ueno A., Tanaka M., Akutagawa M. and Kinouchi Y., 2011. Evaluation of blood flow velocity envelope in common carotid artery for reference data. *Biomedical Signal Processing and Control*, 6(2), 209-215.
- Cutnell J. D. and Johnson, K.W., 1998. *Physics*. Wiley, New York.
- Dong J., Wong K. K. and Tu J., 2013. Hemodynamics analysis of patient-specific carotid bifurcation: A CFD model of downstream peripheral vascular impedance. *International journal for numerical methods in biomedical engineering*, 29(4), 476-491.
- Dunstan D.W., Kingwell B.A., Larsen R., Healy G.N., Cerin E., Hamilton M. T., ... and Owen N., 2012. Breaking up prolonged sitting reduces postprandial glucose and insulin responses. *Diabetes care*, 35(5), 976-983.
- Frostegard J., 2013. Immunity, atherosclerosis and cardiovascular disease. *BMC medicine*, 11(1), 117.
- García-Hermoso A., Martínez-Vizcaíno V., Recio-Rodríguez J.I., Sánchez-López M., Gómez-Marcos M.Á., García-Ortiz L. and EVIDENT Group., 2015. Sedentary behaviour patterns and carotid intima-media thickness in Spanish healthy adult population. *Atherosclerosis*, 239(2), 571-576.
- Glor F.P., Long Q., Hughes A.D., Augst A.D., Ariff B., Thom S.M., ... and Xu X.Y., 2003. Reproducibility study of magnetic resonance image-based computational fluid dynamics prediction of carotid bifurcation flow. *Annals of Biomedical Engineering*, 31(2), 142-151.
- Huynh Q.L., Blizzard C.L., Sharman J.E., Magnussen C.G., Dwyer T. and Venn A.J., 2014. The cross-sectional association of sitting time with carotid artery stiffness in young adults. *BMJ open*, 4(3), e004384.
- Knight J., Olgac U., Saur S.C., Poulidakos D., Marshall W., Cattin P.C., ... and Kurtcuoglu V., 2010. Choosing the optimal wall shear parameter for the prediction of plaque location—a patient-specific computational study in human right coronary arteries. *Atherosclerosis*, 211(2), 445-450.
- Kozáková M., Palombo C., Morizzo C., Nolan J.J., Konrad T. and Balkau B., 2010. Effect of sedentary behaviour and vigorous physical activity on segment-specific carotid wall thickness and its progression in a healthy population. *European heart journal*, 31(12), 1511-1519.
- Ku D.N., Giddens D.P., Zarins C.K. and Glagov S., 1985. Pulsatile flow and atherosclerosis in the human carotid bifurcation. Positive correlation between plaque location and low oscillating shear stress. *Arteriosclerosis, thrombosis, and vascular biology*, 5(3), 293-302.
- Lee S.W., Antiga L., Spence J.D. and Steinman D.A. (2008). Geometry of the carotid bifurcation predicts its exposure to disturbed flow. *Stroke*, 39(8), 2341-2347.
- Lee S.W., Antiga L. and Steinman D.A., 2009. Correlations among indicators of disturbed flow at the normal carotid bifurcation. *Journal of biomechanical engineering*, 131(6), 061013.
- Malek A.M., Alper S.L. and Izumo S., 1999. Hemodynamic shear stress and its role in atherosclerosis. *Jama*, 282(21), 2035-2042.
- Newcomer S.C., Sauder C.L., Kuipers N.T., Laughlin M.H. and Ray C.A., 2008. Effects of posture on shear rates in human brachial and superficial femoral arteries. *American Journal of Physiology-Heart and Circulatory Physiology*, 294(4), H1833-H1839.
- Owen N., Healy G.N., Matthews C.E. and Dunstan D.W., 2010. Too much sitting: the population-health science of sedentary behavior. *Exercise and sport sciences reviews*, 38(3), 105.
- Tu J., Yeoh G.H. and Liu C., 2007. *Computational fluid dynamics: a practical approach*. Butterworth-Heinemann.
- Van de Vosse F. N. and Stergiopoulos N., 2011. Pulse wave propagation in the arterial tree. *Annual Review of Fluid Mechanics*, 43, 467-499.
- Yilmaz F. and Gundogdu M.Y., 2008. A critical review on blood flow in large arteries; relevance to blood rheology, viscosity models, and physiologic conditions. *Korea-Australia Rheology Journal*, 20(4), 197-211.